

## Supporting Information

### Surface Reconstruction of Ni Doped Co-Fe Prussian Blue Analogues for Enhanced Oxygen Evolution

Jingting Hou,<sup>a</sup> Zeming Tang,<sup>a</sup> Keyan Wei,<sup>a</sup> Qingxue Lai <sup>\*a</sup> and Yanyu Liang <sup>\*a</sup>

<sup>a</sup> A Jiangsu Key Laboratory of Materials and Technology for Energy Conversion, College of Materials Science and Technology, Nanjing University of Aeronautics and Astronautics, Nanjing, 210016, P. R. China.

\* E-mail: Laiqingxue@126.com; liangyy403@126.com.

---

## Table of contents

1. Experimental
2. Material Characterizations
3. Electrochemical Measurements
4. Supplementary Figures

**Fig. S1.** SEM images of (a) NiCo-Fe PBAs and (b) Co-Fe PBAs. TEM images of (c) NiCo-Fe PBAs and (d) Co-Fe PBAs.

**Fig. S2.** XPS spectra of (a) Co-Fe PBAs and (b) NiCo-Fe PBAs.

**Fig. S3.** (a) OER polarization curves of Ni<sub>0.8</sub>Co<sub>0.2</sub>-Fe PBAs, Ni<sub>0.6</sub>Co<sub>0.4</sub>-Fe PBAs, Ni<sub>0.4</sub>Co<sub>0.6</sub>-Fe PBAs, Ni<sub>0.2</sub>Co<sub>0.8</sub>-Fe PBAs, Co-Fe PBAs and Ni-Fe PBAs corrected with 95% iR-compensation at a scan rate of 5 mV/s. (b) Volcano plot of all samples by linear fitting.

**Fig. S4.** (a) OER polarization curves and (b) Tafel plots of NiCo-Fe PBAs, Co-Fe PBAs before and after activation.

**Fig. S5.** Overpotentials required for current density at 50 and 100 mA/cm<sup>2</sup> by electrocatalysts.

**Fig. S6.** Nyquist plots of NiCo-Fe PBAs and Co-Fe PBAs.

**Fig. S7.** CV curves of (a) NiCo-Fe PBAs and (b) Co-Fe PBAs with different scan rates.

**Fig. S8.** Chronoamperometry of NiCo-Fe PBAs for (a) 0-5h, (b) 5-15h, (c) 15-35h and (d) 35-40h.

**Fig. S9.** Charge-time plots of NiCo-Fe PBAs obtained from integration of chronoamperometry for (a) 0-5h, (b) 5-15h, (c) 15-35h and (d) 35-40h.

**Fig. S10.** XRD patterns of NiCo-Fe PBAs, Co-Fe PBAs before and after activation.

**Fig. S11.** FT-IR spectra of (a) NiCo-Fe PBAs, (b) Co-Fe PBAs, (c) NiCo-Fe PBAs after activation and (d) Co-Fe PBAs after activation.

**Fig. S12.** XPS spectra of (a) NiCo-Fe PBAs and (b) Co-Fe PBAs after activation.

---

## 1. Experimental

**Materials.** Potassium ferricyanide ( $K_3[Fe(CN)_6]$ ) was purchased from Aladdin Industrial Corporation. Sodium citrate dihydrate ( $C_6H_5Na_3O_7 \cdot 2H_2O$ ) was bought from Sinopharm Chemical Reagent Co., Ltd. Nickel nitrate hexahydrate ( $Ni(NO_3)_2 \cdot 6H_2O$ ) and cobalt nitrate hexahydrate ( $Co(NO_3)_2 \cdot 6H_2O$ ) were purchased from Nanjing Chemical Reagent Co., Ltd. All reagents were used without further purification.

**Synthesis of NiCo-Fe PBAs.** 658.5mg of Potassium ferricyanide was dissolved in 100mL deionized water to form solution A. 1323.5mg of Sodium citrate dihydrate, 174.5mg of nickel nitrate hexahydrate and 697.9mg of cobalt nitrate hexahydrate were dissolved in 100mL deionized water to form solution B, then mix solution A and B with continuous magnetic stirring. After 5min, the mixed solution was aged for 24h at room temperature. washed with water and ethanol for three times to remove the impurities by centrifugation. The NiCo-Fe PBAs were obtained by drying at 60°C for 12h under vacuum. For other ratio of samples, the total amount of nickel nitrate hexahydrate and cobalt nitrate hexahydrate remained unchanged, and adjusted their ratio to 4:6, 6:4 and 8:2.

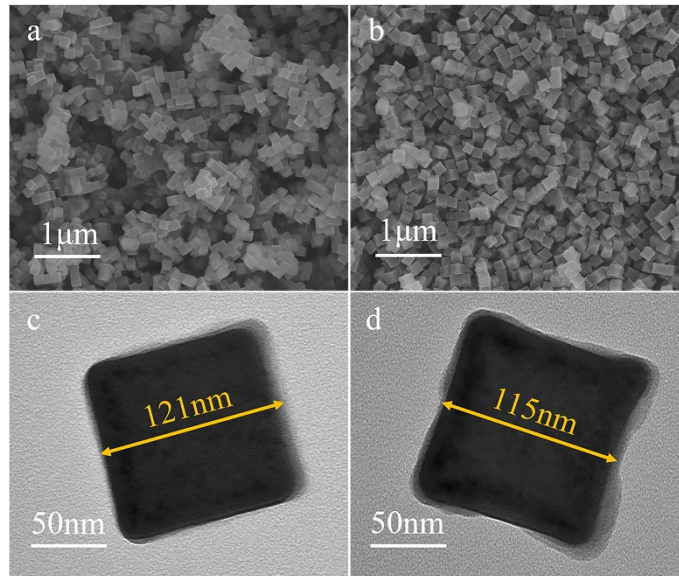
**Synthesis of Co-Fe PBAs.** 658.5mg of Potassium ferricyanide was dissolved in 100mL deionized water to form solution A. 1323.5mg of Sodium citrate dihydrate, 872.4mg of cobalt nitrate hexahydrate were dissolved in 100mL deionized water to form solution B, then mix solution A and B with continuous magnetic stirring. After 5min, the mixed solution was aged for 24h at room temperature. washed with water and ethanol for three times to remove the impurities by centrifugation. The Co-Fe PBAs were obtained by drying at 60°C for 12h under vacuum. For Ni-Fe PBAs, replace cobalt nitrate hexahydrate with nickel nitrate hexahydrate.

## 2. Material Characterizations

The microscopy images, morphology of samples was researched by scanning electron microscopy (SEM, Hitachi S-4800) and transmission electron microscopy (TEM, Philips Tecnai 12). The physical properties of the materials were tested by X-ray diffraction (XRD, ULTRA-55 D5000, Cu  $K\alpha$ ). Fourier transform infrared spectroscopic (FT-IR) was researched by Perkin Elmer Spotlight 300 with KBr pellet method. X-ray photoelectron spectroscopy (XPS) was tested by Kratos AXIS Ultra spectrometer with a source gun of Al  $K\alpha$ .

## 3. Electrochemical Measurements

Electrocatalytic performances of the as-fabricated samples were characterized on CHI660e electrochemical workstation in 1.0 M KOH electrolyte. A Hg/HgO electrode and graphite acted as reference and counter electrodes for OER, respectively. The as-prepared catalysts were supported on Ni foam (1cm $\times$ 4cm) to act as working electrode. 5mg catalyst, 2mg carbon black, 100 $\mu$ L 5wt% Nafion and 900 $\mu$ L ethanol were used to prepare the catalyst slurry. After drying 30 minutes, the slurry was coated on the Ni foam. The working area was tailored to 1cm<sup>2</sup> which is corresponding to the loading mass of about 5mg/cm<sup>2</sup>. Linear sweep voltammetry (LSV) was conducted from 1.0 to 2.0V vs. a reversible hydrogen electrode (RHE) at a scan rate of 0.5mV/s, and all polarization curves were corrected with a 95% iR-compensation. Electrochemical impedance spectroscopy (EIS) was performed over the frequency range of 0.1-100kHz. The stability of the samples was tested by chronopotentiometry measurement at a constant current density of 100mA/cm<sup>2</sup> without iR-compensation. All potentials were converted to RHE though the equation:  $E_{RHE} = E_{(Hg/HgO)} + 0.098 + 0.059 \times pH$ .



#### 4. Supplementary Figures

Fig. S1. SEM images of (a) NiCo-Fe PBAs and (b)Co-Fe PBAs. TEM images of (c) NiCo-Fe PBAs and (d)Co-Fe PBAs.

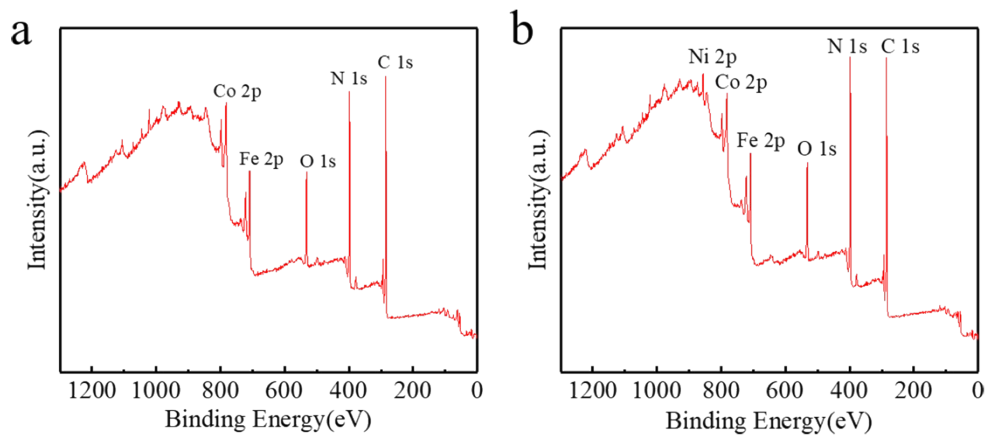


**Fig. S2.** XPS spectra of (a) Co-Fe PBAs and (b) NiCo-Fe PBAs.

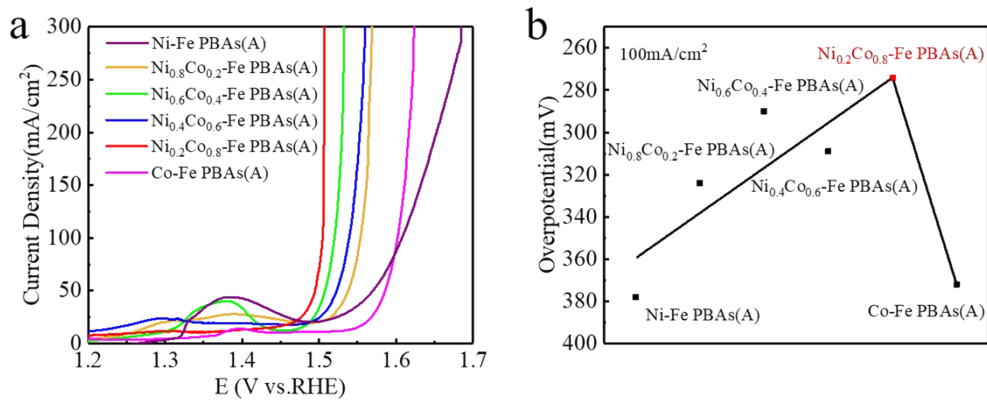


**Fig. S3.** (a) OER polarization curves of Ni<sub>0.8</sub>Co<sub>0.2</sub>-Fe PBAs, Ni<sub>0.6</sub>Co<sub>0.4</sub>-Fe PBAs, Ni<sub>0.4</sub>Co<sub>0.6</sub>-Fe PBAs, Ni<sub>0.2</sub>Co<sub>0.8</sub>-Fe PBAs, Co-Fe PBAs and Ni-Fe PBAs corrected with 95% iR-compensation at a scan rate of 5 mV/s. (b) Volcano plot of all samples by linear fitting.

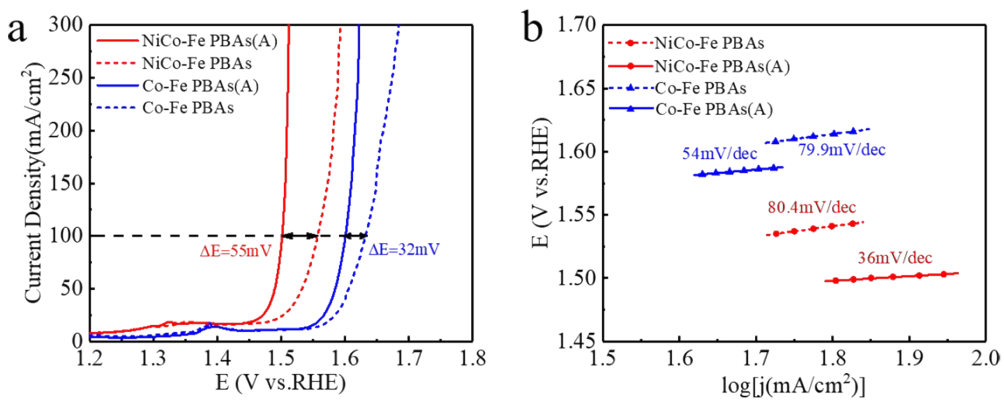


**Fig. S4.** (a) OER polarization curves and (b) Tafel plots of NiCo-Fe PBAs, Co-Fe PBAs before and after activation.

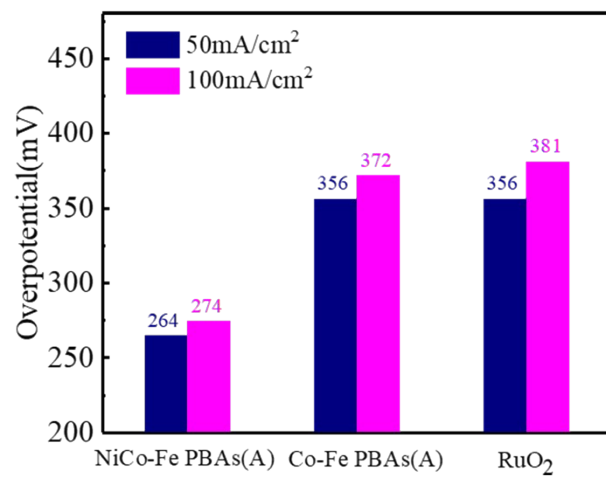


**Fig. S5.** Overpotentials required for current density at 50 and 100 mA/cm<sup>2</sup> by electrocatalysts.



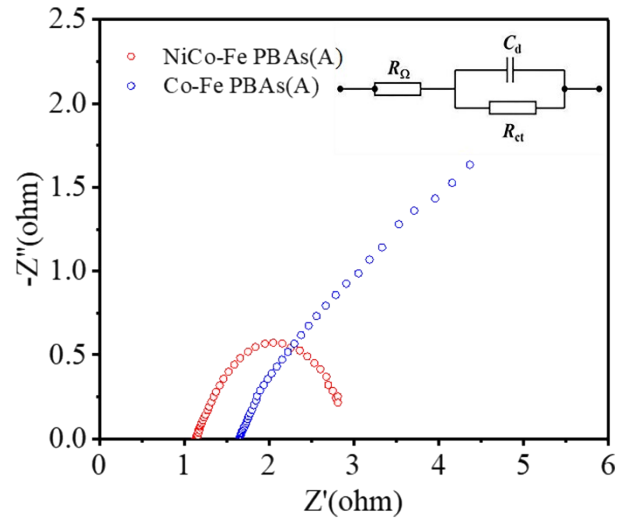
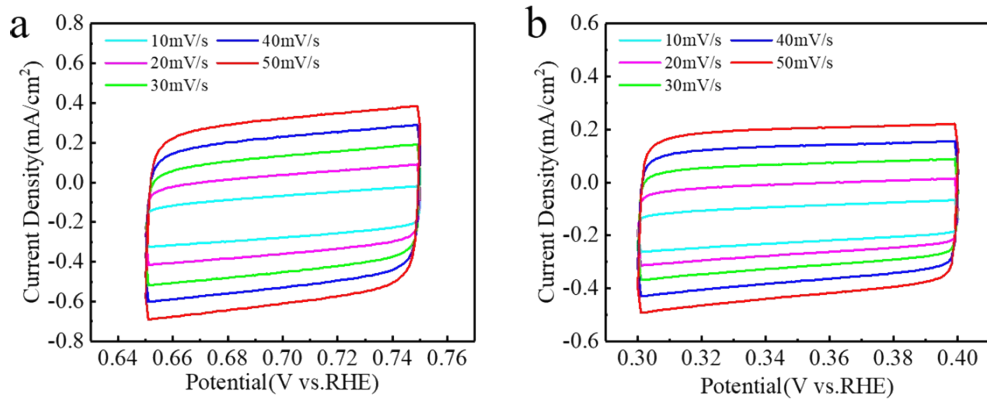
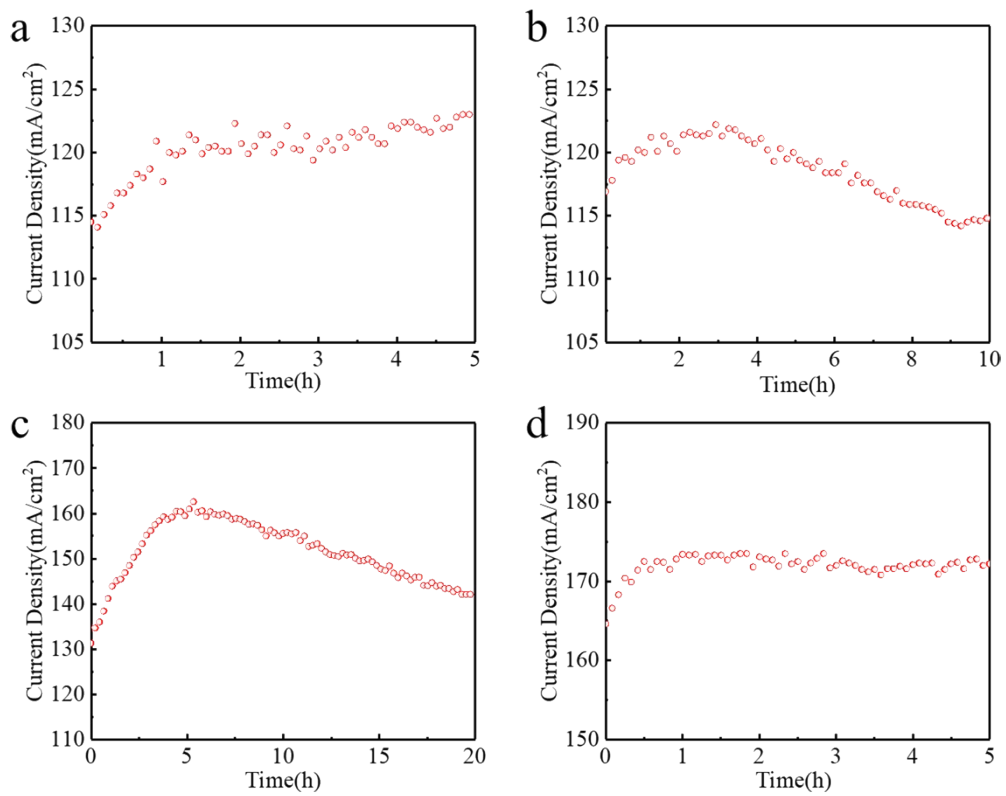


Fig. S6. Nyquis plots of NiCo-Fe PBAs and Co-Fe PBAs.



**Fig. S7.** CV curves of (a) NiCo-Fe PBAs and (b) Co-Fe PBAs with different scan rates.



**Fig. S8.** Chronoamperometry of NiCo-Fe PBAs for (a) 0-5h, (b) 5-15h, (c) 15-35h and (d) 35-40h.

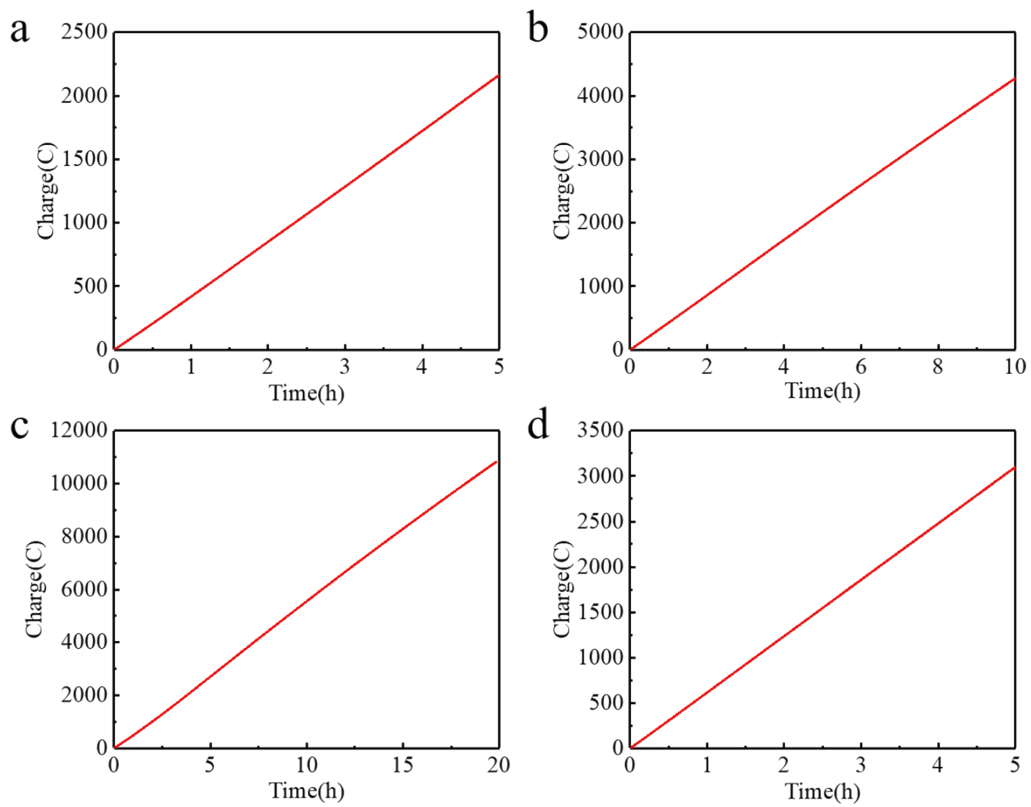


**Fig. S9.** Charge-time plots of NiCo-Fe PBAs obtained from integration of chronoamperometry for (a) 0-5h, (b) 5-15h, (c) 15-35h and (d) 35-40h.

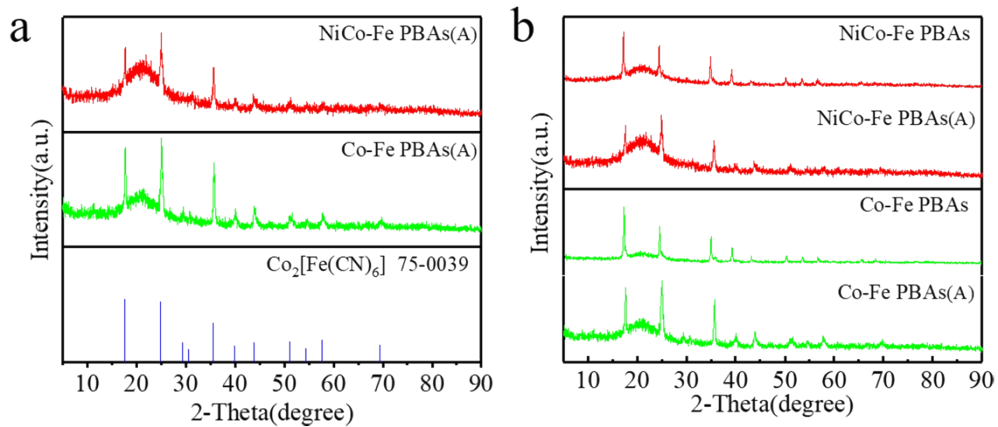


**Fig. S10.** XRD patterns of NiCo-Fe PBAs, Co-Fe PBAs before and after activation.

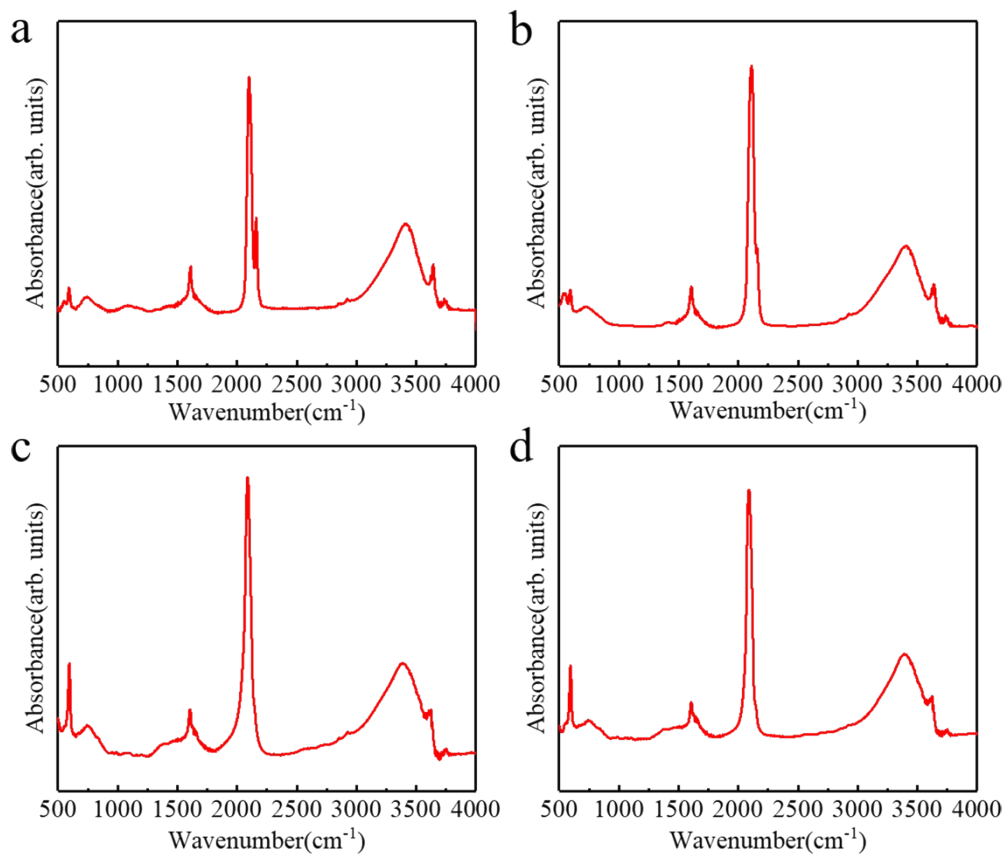


**Fig. S11.** FT-IR spectra of (a) NiCo-Fe PBAs, (b) Co-Fe PBAs, (c) NiCo-Fe PBAs after activation and (d) Co-Fe PBAs after activation.

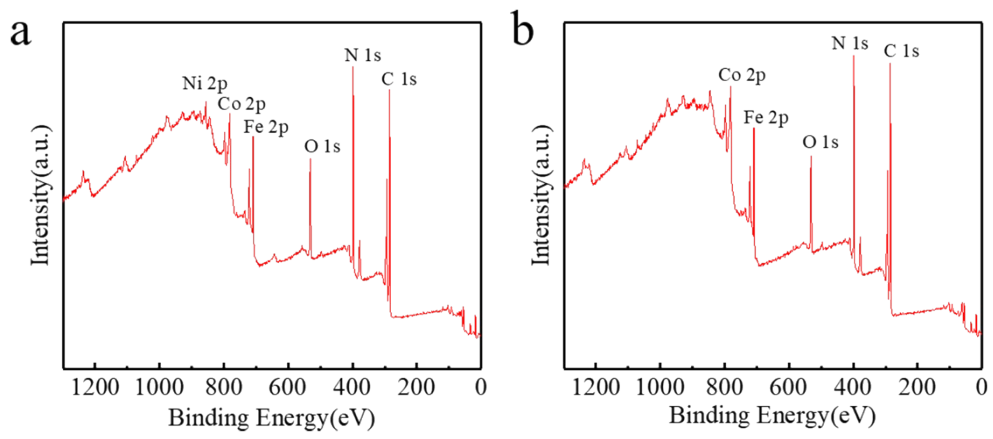


**Fig. S12.** XPS spectra of (a) NiCo-Fe PBAs and (b) Co-Fe PBAs after activation.

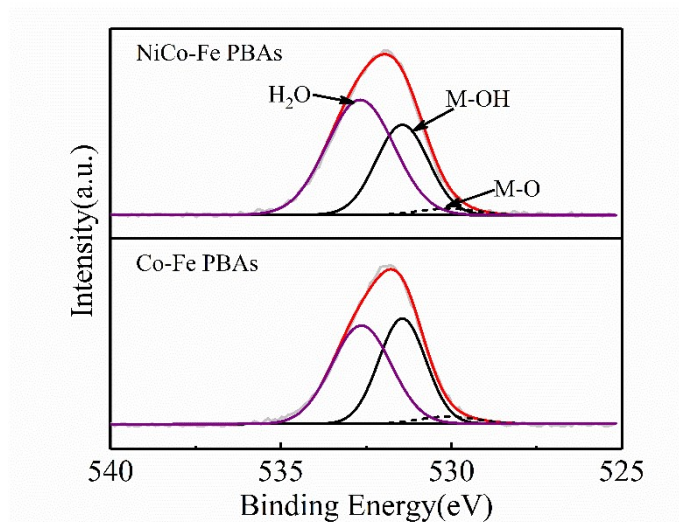


**Fig. S13.** The O 1s spectra of NiCo-Fe PBAs and Co-Fe PBAs.



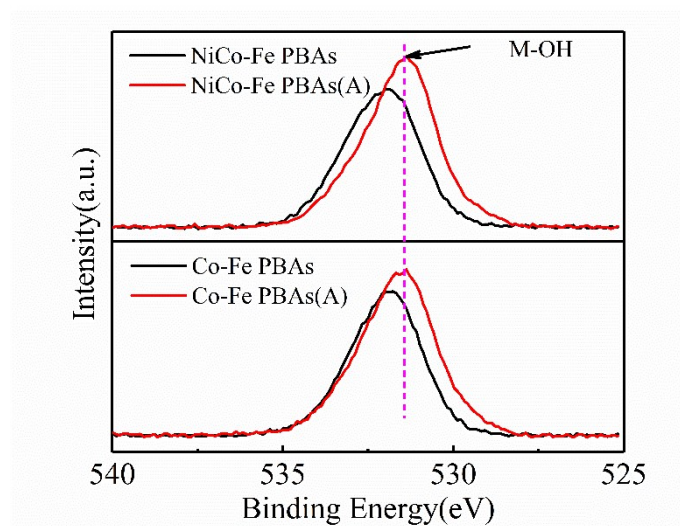


**Fig. S14.** The comparison of O 1s spectra for NiCo-Fe PBAs, Co-Fe PBAs before and after activation.